CO-Releasing Molecules

International Edition: DOI: 10.1002/anie.201502445
German Edition: DOI: 10.1002/ange.201502445

Design, Synthesis, and Functional Evaluation of CO-Releasing Molecules Triggered by Penicillin G Amidase as a Model Protease**

*Nikolay S. Sitnikov, Yingchun Li, Danfeng Zhang, Benito Yard, and Hans-Günther Schmalz**

Abstract: *Protease-triggered CO-releasing molecules (CORMs) were developed. The viability of the approach was demonstrated through the synthesis of compounds consisting of an η^4-oxydiene–$Fe(CO)_3$ moiety connected to a penicillin G amidase (PGA)-cleavable unit through a self-immolative linker. The rate of PGA-induced hydrolysis was investigated by HPLC analysis and the subsequent CO release was quantitatively assessed through headspace gas chromatography. In an in vitro assay with human endothelial cells, typical biological effects of CO, that is, inhibition of the inflammatory response and the induction of heme oxygenase-1 expression, were observed only upon co-administration of the CORM and PGA. This work forms a promising basis for the future development of protease-specific CORMs for potential medicinal applications.*

For a long time, carbon monoxide (CO) was considered to be just a toxic gas that inhibits oxygen transport by red blood cells. However, in the past decade, CO has been identified as an essential biological signaling molecule, which is endogenously produced in humans mainly in the course of heme oxygenase (HO)-catalyzed heme degradation.[1] Given its pronounced anti-inflammatory, cytoprotective, and antihypertensive activity, CO has great therapeutic potential.[2] However, the pharmacological use of gaseous CO is hampered by a high risk of intoxication and a lack of tissue selectivity.[2f,g] To circumvent these problems, CO-releasing molecules (CORMs), mainly based on transition-metal carbonyl complexes, have emerged as potential tools for the in vivo administration of CO.[2a,3] While the first generation CORMs liberate CO (more or less spontaneously) through ligand exchange, there is a demand for CORMs that release CO in vivo in a controlled (preferentially triggered) fashion. As a possible solution, photoactivated CORMs (photo-CORMs)[4] and pH-sensitive CORMs[5] have been developed. Recently, Zobi and co-workers produced a photo-CORM with improved pharmacological properties by conjugating CORM-1 ($[Mn_2(CO)_{10}]$) to vitamin B_{12}.[6]

As a different approach to the development of tissue- or cell-specific CORMs, we recently introduced η^4-acyloxycyclohexadiene–$Fe(CO)_3$ complexes as enzyme-triggered CORMs (ET-CORMs).[7] These compounds release their CO load after activation by a hydrolytic enzyme. The proposed mechanism of CO release is depicted in Scheme 1.

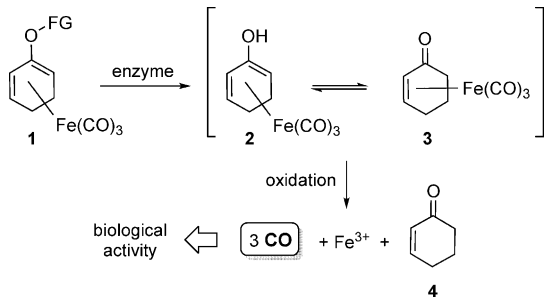

Scheme 1. Proposed activation mechanism of enzyme-triggered CO-releasing molecules (ET-CORMs) of type **1**.

Upon enzymatic cleavage by an esterase, a dienyl ester complex (of type **1**; FG = acyl) is converted into a highly labile dienol–$Fe(CO)_3$ complex intermediate **2**, which disintegrates even under slightly oxidative conditions to afford up to three molecules of CO, as well as a ferric cation (Fe^{3+}) and the dienone ligand **4**.

Having demonstrated the feasibility of the ET-CORM concept with either esterases/lipases or phosphatases as triggers for CO liberation, the development of ET-CORMs activated by specific proteases (peptidases) remained an important challenge since such compounds would enable selective CO delivery to cells displaying enhanced expression of specific proteases.[8] Notably, the up-regulation of proteolytic enzymes is known to be associated with diseases like cancer, rheumatoid arthritis, neurodegenerative disorders, and cardiovascular disorders,[9] all of which are potential targets for CO-based therapy.[2b,f]

The direct attachment of an enzyme-cleavable amide bond to the diene–$Fe(CO)_3$ moiety didn't appear too promising because of the difficult synthetic access and the expected instability of such structures. Moreover, since proteases are much more substrate-specific in comparison to esterases, we reasoned that a close spatial proximity of the amide bond to the bulky and hydrophobic organometallic fragment might hamper hydrolytic cleavage. Therefore, we propose a general

[*] Dr. N. S. Sitnikov, Prof. Dr. H.-G. Schmalz
Department für Chemie, Universität zu Köln
Greinstrasse 4, 50939 Köln (Germany)
E-mail: schmalz@uni-koeln.de
Dr. N. S. Sitnikov
Department of Organic Chemistry
Nizhni Novgorod State University
Gagarina av. 23, 603950 Nizhni Novgorod (Russia)
Y. Li, D. Zhang, Prof. Dr. B. Yard
Medizinische Klinik, Universitätsmedizin Mannheim
Theodor-Kutzer-Ufer 1–3, 68167 Mannheim (Germany)

[**] This research was supported by the University of Cologne within the DFG Excellence Program (UoC Forum). N.S. thanks the Alexander von Humboldt Foundation for a postdoctoral fellowship.

Supporting information for this article is available on the WWW under http://dx.doi.org/10.1002/anie.201502445.

tripartite structure for the protease-activated ET-CORMs comprising 1) a peptidase-specific (oligo-) peptide (the "specifier"), 2) a self-immolative linker,[10] and 3) an oxycyclohexadiene–$Fe(CO)_3$ moiety (Figure 1). After enzymatic

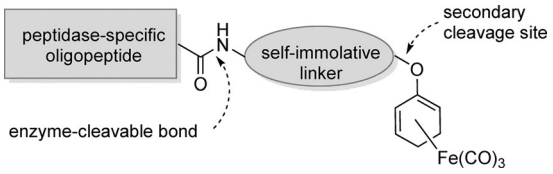

Figure 1. General design of protease-activated ET-CORMs.

cleavage of the specified peptide bond, spontaneous linker elimination would generate the dienol–$Fe(CO)_3$ complex intermediate (**2**), which then undergoes oxidation concomitant with the release of CO. Besides offering the possibility to employ different specifiers, this architecture has the advantage that the CO-release kinetics can be fine-tuned through variation of either the self-immolative linker or the diene–$Fe(CO)_3$ unit. Moreover, the remote positioning of the enzyme-cleavable bond relative to the organometallic moiety should prevent disturbances of the enzymatic hydrolysis step and also suppress kinetic resolution of the "racemic" iron complex unit during the enzymatic reaction. The necessity to control the absolute configuration of the planar chiral diene–$Fe(CO)_3$ moiety can thus be eliminated.

For the proof-of-concept studies reported herein, we selected a *p*-aminobenzyl (PABA)[11] and a "diamine"[12] linker, which differ both in the mechanism of self-immolation (elimination or cyclization) and in the functional group (ether or carbamate) connected to the oxydiene–$Fe(CO)_3$ moiety (Scheme 2).

As a model protease specifier, we chose the phenylacetamide unit, which is reliably recognized and cleaved by penicillin G amidase (PGA).[13] Based on these considerations, four compounds (*rac*-**9** to *rac*-**12**) bearing the oxy substituent either at the "outer" or the "inner" position of the diene–$Fe(CO)_3$ unit were designed (Figure 2).

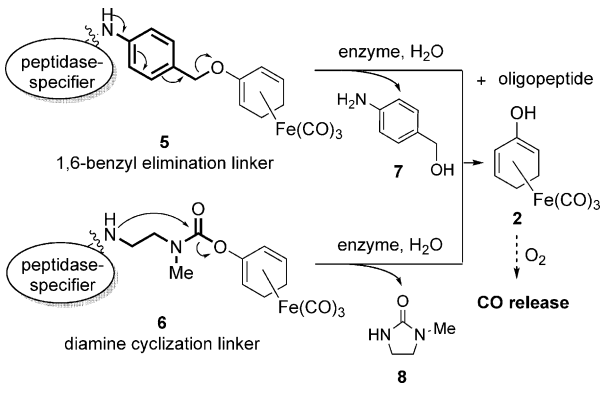

Scheme 2. General structures and cleavage pathways of peptidase-activated ET-CORMs containing self-immolative linkers.

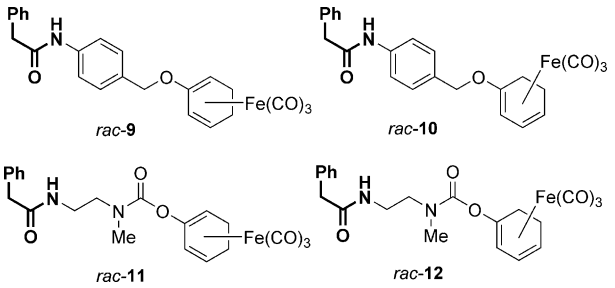

Figure 2. Target complexes *rac*-**9** to *rac*-**12**, which contain a PGA-cleavable moiety.

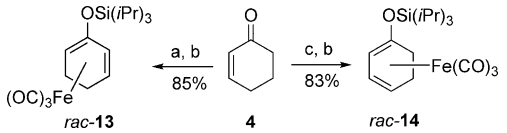

Scheme 3. Synthesis of starting complexes *rac*-**13** and *rac*-**14** according to Ref. [7c]. a) LDA, THF, −78 °C, 1 h; then $(iPr)_3SiOTf$, −78 °C to RT, 1 h. b) $[Fe_2(CO)_9]$, Et_2O, reflux, 16 h. c) LiHMDS, TPPA, THF, −78 °C, 1 h; then $(iPr)_3SiOTf$, −78 °C to room temperature, 1 h. LDA = lithium diisopropylamide, THF = tetrahydrofuran, LiHMDS = lithium hexamethyldisilazane, TPPA = tripyrrolidinophosphoric acid triamide.

First, the isomeric TIPS-protected dienol–$Fe(CO)_3$ building blocks *rac*-**13** and *rac*-**14** were prepared from cyclohexenone (**4**) as previously described (Scheme 3).[7c]

The synthesis of *rac*-**9** commenced with the conversion of *p*-aminobenzylic alcohol (**7**) into the phenylacetamide **15** and subsequent conversion of the benzylic alcohol into a bromide (**16**) under Corey–Kim conditions[14] (Scheme 4). After purification, **16** was reacted with the dienolate–$Fe(CO)_3$complex *rac*-**17**, which was generated in situ from *rac*-**13** with TBAF/NaH in THF, to smoothly afford *rac*-**9**.

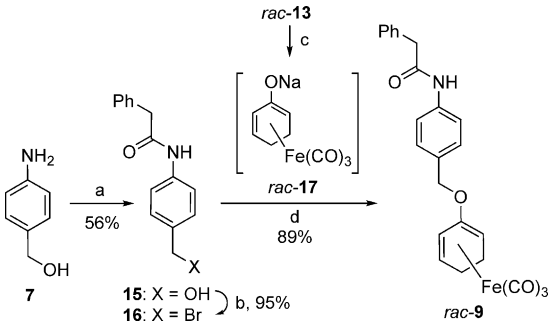

Scheme 4. Synthesis of *rac*-**9**. a) Phenylacetyl chloride, pyridine, CH_2Cl_2/DMF (8:1, v/v), RT, 12 h. b) NBS, Me_2S, CH_2Cl_2, 0 °C to room temperature, 12 h. c) TBAF, NaH, THF, 0 °C, 10 min. d) THF, 0 °C to RT, 1 h. DMF = *N*,*N*-dimethylformamide, NBS = *N*-bromosuccinimide, TBAF = tetrabutylammonium fluoride.

The synthesis of *rac*-**10** as the second target structure was attempted under the same conditions. However, when **16** was reacted with the dienolate–$Fe(CO)_3$ complex *rac*-**18** (generated in situ from *rac*-**14**), only compounds **19**–**21** were formed as major products, while no traces of *rac*-**10** could be isolated (Scheme 5). Other attempts to achieve the synthesis of *rac*-**10**

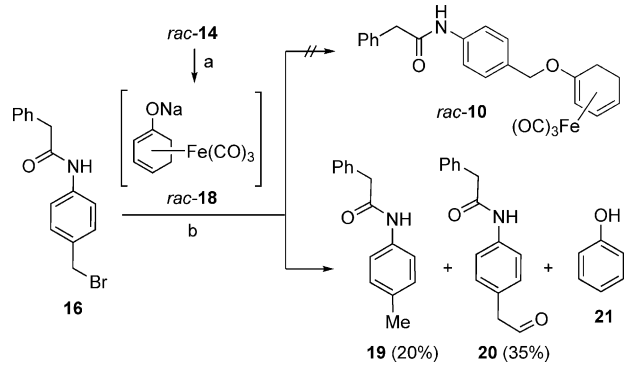

Scheme 5. Attempted synthesis of *rac*-**10**. a) TBAF, NaH, THF, 0 °C, 10 min. b) THF, 0 °C to RT, 24 h.

by using TPPA as a cosolvent or by employing different electrophiles (such as the mesylate or the trichloroacetimidate derived from **15**) also failed.[15]

Next, we turned our attention to the synthesis of the carbamate target molecules *rac*-**11** and *rac*-**12**. For this purpose, *N*-methyl-ethylenediamine was first converted into the amide **24** through regioselective monoacylation with methyl phenylacetate in the presence of 1,5,7-triazabicyclo-[4.4.0]dec-5-ene.[16] The target complexes *rac*-**11** and *rac*-**12**, were then obtained through the reaction of **24** with the mixed carbonates *rac*-**22** and *rac*-**23** (generated from *rac*-**13** and *rac*-**14**), respectively, through desilylation with TBAF and trapping the in situ formed dienolate complexes with *p*-nitrophenyl chloroformate. Both target compounds (*rac*-**11** and *rac*-**12**) were obtained in good yield in a three-step one-pot sequence (Scheme 6).

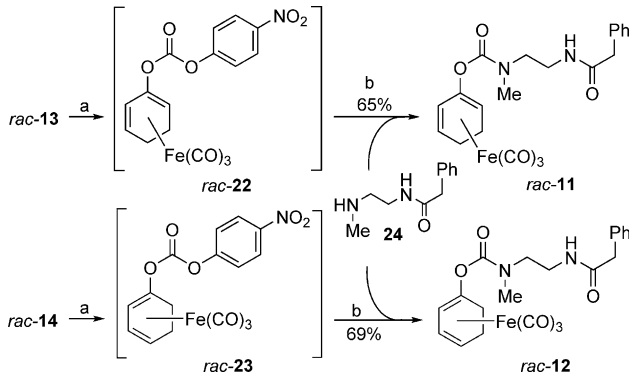

Scheme 6. Synthesis of complexes *rac*-**11** and *rac*-**12**. a) TBAF, THF, 0 °C, 10 min; then 4-nitrophenyl chloroformate, 0 °C, 40 min. b) THF, pyridine, 0 °C to RT, 12 h.

The final goal of our study was to probe the ability of the prepared compounds (*rac*-**9**, *rac*-**11**, and *rac*-**12**) to release CO upon activation by PGA. The enzyme-triggered reaction cascade comprises three steps, which all are expected to contribute to the overall rate of carbon monoxide generation. These are 1) enzymatic hydrolysis of the phenylacetamide unit, 2) linker self-immolation to form the sensitive dienol–$Fe(CO)_3$ intermediate, and 3) oxidation-induced disintegration of the latter to release CO.

The rates of PGA-mediated hydrolysis and linker self-immolation for *rac*-**9**, *rac*-**11**, and *rac*-**12** were investigated by reversed-phase HPLC analysis. For this purpose, a solution of the studied compound (1 μmol) in DMSO (100 μL) was added along with PGA (4 μL for *rac*-**9**; 2 μL for *rac*-**11** and *rac*-**12**) to degassed Sorensen's phosphate buffer (50 mM, pH 7.8, 1.9 mL) preheated to 37 °C. The reaction mixture was stirred at 37 °C for 24 h and aliquots were taken occasionally for analysis (see the Supporting Information). In control experiments performed under identical conditions, none of the compounds underwent any hydrolysis within 24 h in the absence of the enzyme. In the case of *rac*-**9**, three peaks corresponding to the starting material, the deacylated intermediate *rac*-**25**, and the dienol–$Fe(CO)_3$ complex *rac*-**2** were observed in the presence of PGA (Figure 3). This allowed us to monitor the concentration changes for all three species in a time-resolved manner (Figure 4). The half-life of *rac*-**9** was 5 h under these conditions.

As shown in Figure 4, the rates of enzymatic hydrolysis and linker self-immolation are comparable, with both contributing to the rate of *rac*-**2** formation from *rac*-**9**. Notably, HPLC measurements with a chiral stationary phase indicated only minor kinetic resolution during the enzymatic hydrolysis of *rac*-**9**, with a maximum of 6 % *ee* (**9**/*ent*-**9**) after 1 h.

In contrast to *rac*-**9**, both PGA-mediated hydrolysis and subsequent linker immolation were found to be rapid for *rac*-

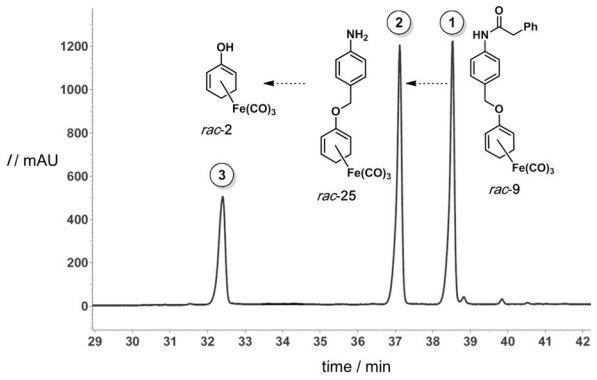

Figure 3. HPLC chromatogram of the PGA-catalyzed hydrolysis of *rac*-**9** after incubation for 6 h. Peaks 1, 2, and 3 correspond to the compounds *rac*-**9**, *rac*-**25**, and *rac*-**2** respectively.

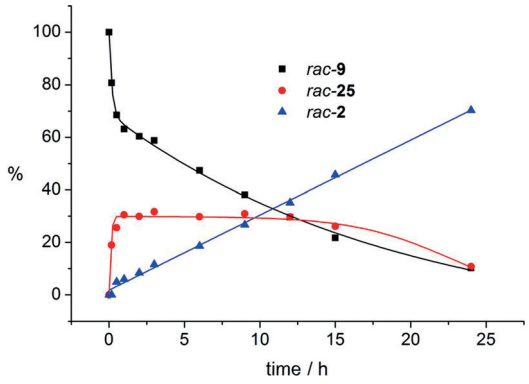

Figure 4. Monitoring PGA-catalyzed hydrolysis and linker elimination for compound *rac*-**9** by RP-HPLC.

11 and *rac*-**12** under the standard conditions. For both of these substrates, a complete conversion to *rac*-**2** (or the respective external isomer) was observed within 10 min and no intermediate could be detected by HPLC analysis.

Quantitative assessment of CO release from *rac*-**9**, *rac*-**11**, and *rac*-**12** associated with cleavage of the amide bond was performed by using headspace GC (for details, including the calibration procedure, see the Supporting Information). To ensure the build-up of sufficiently high concentrations of CO in the gas phase, the reactions were performed at higher concentrations. A solution of the studied compound (10 μmol) in DMSO (100 μL) was added along with PGA (40 μL for *rac*-**9** and 20 μL for *rac*-**11** or *rac*-**12**) to Sorensen's phosphate buffer (50 mM, pH 7.8, 1.9 mL) preheated to 37 °C in a 10 mL GC vial. After sealing the vial with a rubber septum, the mixture was stirred at 37 °C for 96 h and the gas phase was periodically sampled for analysis.

While control experiments clearly showed that no CO was generated in the absence of added enzyme, PGA-triggered CO release could be clearly detected for all three substrates. Interestingly, the release of CO from *rac*-**9** proceeded at a comparably slow rate compared to the substrates containing a diamine linker (*rac*-**11** and *rac*-**12**; Figure 5).

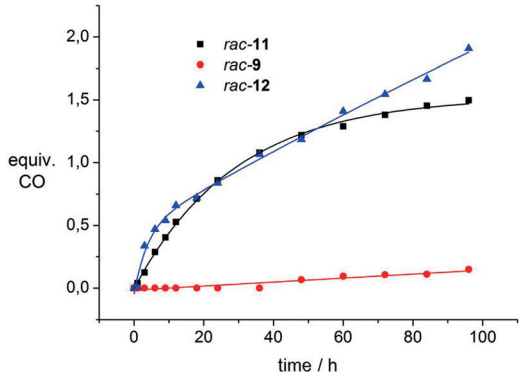

Figure 5. PGA-triggered CO release from compounds *rac*-**9**, *rac*-**11**, and *rac*-**12**, as determined by headspace gas chromatography.

Having proven the general ability of *rac*-**9**, *rac*-**11**, and *rac*-**12** to act as PGA-triggered CO-releasing molecules, we next probed whether such compounds also produce CO-associated biological effects in vitro. For this purpose, human umbilical vein endothelial cells (HUVECs) were stimulated with the pro-inflammatory cytokine TNF-α and the ability of *rac*-**9** (12.5 μL) to alter the expression of vascular cell adhesion molecule-1 (VCAM-1) and heme oxygenase-1 (HO-1) with/without the addition of PGA as a trigger enzyme was assessed by western blot analysis.[17]

Effective inhibition of VCAM-1 expression as well as induction of HO-1, was observed only in the presence of both *rac*-**9** and PGA, while in the control experiments (with TNF-α alone or with TNF-α/*rac*-**9** in the absence of PGA) a normal inflammatory response was observed (Figure 6). Notably, *rac*-**9** did not display significant levels of cytotoxicity towards HUVECs at the concentration used (half maximal effective concentration (EC_{50}) > 50 μM).

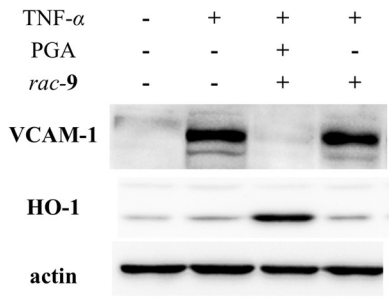

Figure 6. Western blot analysis of VCAM-1 and HO-1 expression in HUVEC cells incubated for 24 h in the presence (+) or absence (−) of TNF-α (50 ng mL^{-1}), PGA (1 U mL^{-1}; ca. 3 nM), and *rac*-**9** (12.5 μmol L^{-1}). To confirm equal protein loading, the membranes were re-probed with a monoclonal antibody against β-actin.

In conclusion, with the aim of developing protease-triggered CORMs, we designed and successfully synthesized a first series of oxydiene–Fe(CO)$_3$ complexes with a PGA-cleavable side chain connected to the organometallic unit through either a *p*-aminobenzyl (*rac*-**9**) or a *N*-methyl-1,2-ethylenediamincarbonyl unit (*rac*-**11**, *rac*-**12**) as a self-immolative linker. As a proof of concept, we demonstrated that upon amidase-induced cleavage of the amide bond, these model substrates indeed undergo the expected decay, thereby leading to the release of CO. The PGA-induced liberation of CO was also demonstrated for *rac*-**9** in a cell-based assay. We are therefore optimistic that the concept disclosed herein could be exploited for the future development of enzyme-triggered CO-releasing molecules (ET-CORMs) with more advanced protease specifiers, which would enable tissue-specific CO release in response to the presence of disease-relevant proteases. In this context, different linkers (e.g., elongated diamine linkers[18] or PABA units with additional substituents[19]) might also be used to fine-tune the rate of CO release and other pharmacological properties.

Keywords: carbon monoxide · carbonyl complexes · enzyme catalysis · iron · organometallic compounds

How to cite: *Angew. Chem. Int. Ed.* **2015**, *54*, 12314–12318
Angew. Chem. **2015**, *127*, 12489–12493

[1] a) R. Motterlini, R. Foresti, *Antioxid. Redox Signaling* **2014**, *20*, 1810–1826; b) P. A. Dennery, *Antioxid. Redox Signaling* **2014**, *20*, 1743–1753; c) S. W. Ryter, J. Alam, A. M. K. Choi, *Physiol. Rev.* **2006**, *86*, 583–650; d) M. D. Maines, *Annu. Rev. Pharmacol. Toxicol.* **1997**, *37*, 517–554.

[2] a) S. H. Heinemann, T. Hoshi, M. Westerhausen, A. Schiller, *Chem. Commun.* **2014**, *50*, 3644–3660; b) L. Rochette, Y. Cottin, M. Zeller, C. Vergely, *Pharmacol. Ther.* **2013**, *137*, 133–152; c) F. Gullotta, A. di Masi, P. Ascenzi, *Iubmb Life* **2012**, *64*, 378–386; d) S. Ghosh, J. Gal, N. Marczin, *Ann. Med.* **2010**, *42*, 1–12; e) B. E. Mann, *Top. Organomet. Chem.* **2010**, *32*, 247–285; f) R. Motterlini, L. E. Otterbein, *Nat. Rev. Drug Discovery* **2010**, *9*, 728–743; g) R. Foresti, M. G. Bani-Hani, R. Motterlini, *Intensive Care Med.* **2008**, *34*, 649–658; h) L. Y. Wu, R. Wang, *Pharmacol. Rev.* **2005**, *57*, 585–630.

[3] a) S. García-Gallego, G. J. L. Bernardes, *Angew. Chem. Int. Ed.* **2014**, *53*, 9712–9721; *Angew. Chem.* **2014**, *126*, 9868–9877; b) F. Zobi, *Future Med. Chem.* **2013**, *5*, 175–188; c) C. C. Romão,

W. A. Blaettler, J. D. Seixas, G. J. L. Bernardes, *Chem. Soc. Rev.* **2012**, *41*, 3571 – 3583; d) B. E. Mann, *Organometallics* **2012**, *31*, 5728 – 5735; e) M. J. Alcaraz, M. I. Guillen, M. L. Ferrandiz, J. Megias, R. Motterlini, *Curr. Pharm. Des.* **2008**, *14*, 465 – 472; f) R. Alberto, R. Motterlini, *Dalton Trans.* **2007**, 1651 – 1660.

[4] a) M. A. Gonzales, P. K. Mascharak, *J. Inorg. Biochem.* **2014**, *133*, 127 – 135; b) U. Schatzschneider, *Inorg. Chim. Acta* **2011**, *374*, 19 – 23.

[5] T. S. Pitchumony, B. Spingler, R. Motterlini, R. Alberto, *Org. Biomol. Chem.* **2010**, *8*, 4849 – 4854.

[6] F. Zobi, L. Quaroni, G. Santoro, T. Zlateva, O. Blacque, B. Sarafimov, M. C. Schaub, A. Y. Bogdanova, *J. Med. Chem.* **2013**, *56*, 6719 – 6731.

[7] a) S. Romanski, B. Kraus, U. Schatzschneider, J.-M. Neudoerfl, S. Amslinger, H.-G. Schmalz, *Angew. Chem. Int. Ed.* **2011**, *50*, 2392 – 2396; *Angew. Chem.* **2011**, *123*, 2440 – 2444; b) S. Romanski, H. Ruecker, E. Stamellou, M. Guttentag, J.-M. Neudoerfl, R. Alberto, S. Amslinger, B. Yard, H.-G. Schmalz, *Organometallics* **2012**, *31*, 5800 – 5809; c) S. Romanski, B. Kraus, M. Guttentag, W. Schlundt, H. Ruecker, A. Adler, J.-M. Neudoerfl, R. Alberto, S. Amslinger, H.-G. Schmalz, *Dalton Trans.* **2012**, *41*, 13862 – 13875; d) S. Romanski, E. Stamellou, J. T. Jaraba, D. Storz, B. K. Kraemer, M. Hafner, S. Amslinger, H.-G. Schmalz, B. A. Yard, *Free Radical Biol. Med.* **2013**, *65*, 78 – 88; e) E. Stamellou, D. Storz, S. Botov, E. Ntasis, J. Wedel, S. Sollazzo, B. K. Kramer, W. van Son, M. Seelen, H.-G. Schmalz, A. Schmidt, M. Hafner, B. A. Yard, *Redox biol.* **2014**, *2*, 739 – 748.

[8] a) K. Y. Choi, M. Swierczewska, S. Lee, X. Chen, *Theranostics* **2012**, *2*, 156 – 178; b) U. H. Weidle, G. Tiefenthaler, G. Georges, *Cancer Genomics Proteomics* **2014**, *11*, 67 – 79; c) D. Gabriel, M. F. Zuluaga, H. van den Bergh, R. Gurny, N. Lange, *Curr. Med. Chem.* **2011**, *18*, 1785 – 1805.

[9] C. Lopez-Otin, J. S. Bond, *J. Biol. Chem.* **2008**, *283*, 30433 – 30437.

[10] a) F. Kratz, I. A. Muller, C. Ryppa, A. Warnecke, *ChemMedChem* **2008**, *3*, 20 – 53; b) Y. Meyer, J.-A. Richard, B. Delest, P. Noack, P.-Y. Renard, A. Romieu, *Org. Biomol. Chem.* **2010**, *8*, 1777 – 1780.

[11] a) P. L. Carl, P. K. Chakravarty, J. A. Katzenellenbogen, *J. Med. Chem.* **1981**, *24*, 479 – 480; b) J. A. Richard, Y. Meyer, V. Jolivel, M. Massonneau, R. Dumeunier, D. Vaudry, H. Vaudry, P. Y. Renard, A. Romieu, *Bioconjugate Chem.* **2008**, *19*, 1707 – 1718; c) J. A. Richard, L. Jean, C. Schenkels, M. Massonneau, A. Romieu, P. Y. Renard, *Org. Biomol. Chem.* **2009**, *7*, 2941 – 2957.

[12] W. S. Saari, J. E. Schwering, P. A. Lyle, S. J. Smith, E. L. Engelhardt, *J. Med. Chem.* **1990**, *33*, 97 – 101.

[13] a) A. K. Chandel, L. V. Rao, M. L. Narasu, O. V. Singh, *Enzyme Microb. Technol.* **2008**, *42*, 199 – 207.

[14] E. J. Corey, C. U. Kim, M. Takeda, *Tetrahedron Lett.* **1972**, *13*, 4339 – 4342.

[15] For a mechanistic rationale of this reaction outcome, see the Supporting Information.

[16] C. Sabot, K. A. Kumar, S. Meunier, C. Mioskowski, *Tetrahedron Lett.* **2007**, *48*, 3863 – 3866.

[17] Although compounds *rac*-**11** and *rac*-**12** showed fast PGA-induced CO release (as assessed by headspace GC), initial experiments with endothelial cells indicated that they inhibit VCAM-1 expression in a partly PGA-independent manner. Since the reason for this unexpected behavior is unknown (it is currently being investigated), we focused on compound *rac*-**9**, which produces the characteristic biological effects of CO-release in a clearly PGA-dependent manner.

[18] F. M. H. de Groot, W. J. Loos, R. Koekkoek, L. W. A. van Berkom, G. F. Busscher, A. E. Seelen, C. Albrecht, P. de Bruijn, H. W. Scheeren, *J. Org. Chem.* **2001**, *66*, 8815 – 8830.

[19] K. M. Schmid, L. Jensen, S. T. Phillips, *J. Org. Chem.* **2012**, *77*, 4363 – 4374.

Received: March 16, 2015
Revised: April 24, 2015
Published online: June 2, 2015

